

ORIGINAL ARTICLE**Omentin -1 antagonizes High Fat Induced Bone Loss in Rats and Promotes Bone Growth via AMPK/mTORC1/ PPAR- γ and GDF-11 Signaling Pathway**Nanees F. El-Malkey¹, Nisreen E. Elwany*², Nehal I. A. Goda³, Mohamed Aref⁴, Sama S. Khalil¹¹ Medical Physiology Department, Faculty of Medicine, Zagazig University, Zagazig, Sharkia, Egypt² Clinical Pharmacology Department, Faculty of Medicine, Zagazig University, Zagazig, Sharkia, Egypt.³ Department of Histology and Cytology, Faculty of Veterinary Medicine, Zagazig University, Zagazig, Egypt⁴ Anatomy Department, Faculty of Veterinary Medicine, Zagazig University, Zagazig, Sharkia, Egypt.**Corresponding author:**

Nisreen E. Elwany

E-mail:

Nisreenelwany@yahoo.com

Submit Date 2023-04-30 16:08:37

Revise Date 2023-05-27 21:08:15

Accept Date 2023-05-31

ABSTRACT

Background: Obesity induces bone related diseases as a consequence of reduced bone formation and unwarranted bone resorption. Therefore, the possible impact of adipokines on osteogenesis has been considered. Nevertheless, the osteogenic properties of omentin-1 are indistinct and contentious. The objective of the current work was to determine the regulatory effects of omentin-1 on bone turnover, along with exploring the fundamental molecular mechanisms in obese rats. **Methods:** The present study investigated the effects of intraperitoneal omentin-1 injection (8 μ g/kg, once daily, for 14 days) in rats after feeding a high-fat diet for 10 weeks to induce obesity. Metabolic parameters and bone dry and ash weights were measured; serum calcium, phosphorus, alkaline phosphatase, and growth differentiation factor-11 (GDF-11), and femur histopathological changes were analyzed. Additionally, we investigated the effect of omentin-1 treatment on AMP protein-kinase (AMPK), mammalian target rapamycin (mTORC1) and nuclear receptor peroxisome proliferator-activated receptor- γ (PPAR- γ) expression. **Results:** The results revealed significant improvement in metabolic, bone biochemical parameters and histopathological changes in the omentin-1 treated group with a significant increase in area % of bone. A significant down-regulation of mTORC1 was identified through AMPK/mTORC1/PPAR- γ pathway accompanied by an increase in serum GDF-11. **Conclusions:** Omentin-1 can significantly promote bone health and viability via down-regulation of the AMPK/mTORC1/PPAR- γ signaling pathway and up-regulation of serum GDF-11, thus it can promote bone formation and prevent osteoporosis.

Keywords: Obesity, Omentin-1, GDF-11, mTORC1, Rats.

**INTRODUCTION**

Osteoporosis and obesity are interrelated metabolic derangements, which are serious and prevalent health issues [1]. Osteoporosis is a systemic bone disorder that is characterized by a diminution in bone mass and worsening of the bone microstructure [2].

Obesity is one of the most significant risk factors for chronic illnesses, such as metabolic syndrome, type 2 diabetes mellitus (T2DM) and cardiovascular issues. It has been reported that consuming rats and mice a high-fat diet (HFD) during the time of growth has negative impacts on bone metrics [3].

Obesity boosts bone marrow adipogenesis, while inhibiting osteoblastogenesis adipocytes and osteoblasts are both generated from multipotent mesenchymal stem cells, through

various pathways, including transforming growth factor (TGF) signaling, the RANKL/RANK/osteoprotegerin (OPG) pathway and the peroxisome proliferator-activated receptor gamma (PPAR- pathway), which can modulate bone cell metabolism both in vitro and in vivo, cytokines derived from adipose tissue also appear to play a significant role in bone metabolism [4].

Mammalian target of rapamycin (mTOR) is a serine/threonine protein kinase related to phosphoinositol-3-kinases (PI3K) that controls cellular development and metabolism in response to alterations in hormone and nutrition levels [5]. Obesity and T2DM are neurodegenerative diseases that have all been related to the pathophysiology of several human ailments by dysregulation of mTOR signaling [6].

Although the impact of mTOR signaling on bone turnover has been extensively studied, the clinical uses of mTOR activators and inhibitors for treating osteoporosis have not been well established [7].

Omentin-1 is a hydrophilic adipokine with 313 amino acids that is only expressed in omental adipose tissue and is widely present in plasma. Omentin-1 has been shown to have a key role in a number of physiological processes, such as insulin action, cardiovascular function and the inflammatory response [8]. Omentin-1 may play crucial roles in the regulation of bone metabolism, but the results have been inconsistent. Several studies showed that high omentin-1 protected from osteoporosis by suppressing bone resorption and promoting bone formation in mice [9]. Other studies showed that serum levels of omentin-1 were negatively correlated with bone mineral density (BMD) and bone turnover markers through inhibiting bone formation in diabetic osteoporosis and postmenopausal women [10], others showed that omentin-1 has no effect on bone metabolism [11]. Nonetheless, the osteogenic outcome induced by omentin-1 remains uncertain [12].

Bone morphogenetic protein 11 is another name for growth differentiation factor 11(GDF11). A number of the TGF-members including the GDF11, were in charge of planning bone remodeling. In order to control the remodeling of bones, TGF encourages osteoclast depressive development. Moreover, TGF-promotes the production of osteoclasts [13]. However, it is unclear how GDF-11 contributes to the emergence of obesity and metabolic diseases associated with it [14].

As the effects and mechanisms of omentin-1 on bone metabolism in vivo remain unknown, we aimed in this study to clarify the biological roles of omentin-1 in the high fat diet (HFD)-induced bone loss and to explore the relationship between omentin-1 and the DGF-11 for revealing the new mechanism of omentin-1 function.

SUBJECT AND METHODS

The animal house at Zagazig University's faculty of medicine served as the site of the current study. A total of 30 healthy adult male albino rats of the local breed, weighing (210± 10.15 grams), were used. According to the Institute of Laboratory Animal Resources, all animals received care that was compliant with animal care and ethical standards (1996). The study's protocol was approved by Zagazig University's institutional animal care and use

committee. ZU-IACUC/3/F/183/2022 is the approval number.

Throughout the course of the trial, all animals were kept in sanitary conditions in plastic cages (50× 60× 60cm, 5 rats/cage); with free access to food and water, a pleasant temperature (22°C), and regular light and dark cycles.

Study design

The rats were split into two groups after two weeks of acclimatization; group I, the vehicle-treated control group (n=10), consisted of animals fed a conventional chow diet (5% of energy came from fat, 18% from proteins and 77% from carbs; 3.3kcal/g).After 10 weeks; 0.2 ml of physiologic saline was injected intraperitoneally (i.p) into each rat every day for 14 days.

Group II (n=20): Rats were fed a high fat diet (HFD) consisting of 60% fat, 21% carbohydrate, 18% protein, and 5.1 calories/g (Faculty of Veterinary Medicine, Zagazig University) for 10 weeks in order to develop obesity [15]; after which, they were randomly split into two subgroups (each with n=10); The obese control group (obese subgroup IIa): For 14 days in a row, 0.2 ml of physiologic saline was injected i.p into each rat and in the Omentin subgroup (IIb) (Omentin-1 treated obese), each rat received 8µg/kg of rat omentin-1 for 14 days in a row (SRP8047-10 UG/vial, purchased from Sigma-Aldrich Co., Saint Louis), which was diluted in saline and administered i.p [16].Body mass index and biochemical analysis were performed following the final Omentin-1 injection, the following procedures were carried out, 24 hours later.

Calculating Body Mass Index (BMI)

Body mass index (BMI) is equals to body weight (g)/length² (cm²). BMI is used as an indicator of obesity where the cut off value of obesity BMI is more than 0.68g/cm² [17]

Blood analysis

Blood samples were collected from retro-orbital venous plexus while the animal was anesthetized by Ketamine- Xylaject Hcl Mixture at ratio 2:1(1mL/ Kg) and serum was separated by centrifugation of clotted blood, then kept deep frozen at -80°C until biochemical serum analysis for the following parameters were done:

- Serum glucose level: According to Tietz et al. [18] using glucose enzymatic (GOD-PAP)-liquizyme Kits (Biotechnology, Egypt).
- Serum insulin level: By a solid phase enzyme amplified sensitivity immunoassay according to Temple et al.[19] using Enzyme Amplified

Sensitivity Immunoassay Kits (Bio Source Europe S.A., Belgium).

-Homeostasis model assessment of insulin resistance (HOMA-IR) was assessed as follow: "HOMA-IR= insulin ($\mu\text{U/mL}$) x glucose (mg/dL)/405".

- Serum total cholesterol (TC) level and triglycerides (TG) level: According to Tietz et al.[18] using the corresponding rat enzyme-linked immunosorbent assay kit, (Bio Source Europe S.A.-Rue de l'Industrie, 8-B- 1400 Nivelles-Belgium).

- Serum calcium (Ca) and inorganic phosphorus (IP) were measured by an automatic biochemical analyzer (Oriental Yeast Co., Ltd., Tokyo, Japan). Moreover, alkaline phosphatase (ALP) activity was assayed according to Farley et al.[20].

- Serum GDF11 concentrations were determined using a rat ELISA kit (BioSource Europe S.A., Belgium) according to Juan et al. [21].

Macro morphological examination

After blood samples were taken, the animals were killed by Cervical dislocation (CD) under anesthesia, placed in a ventrodorsal position, and the skin of the hind limbs was then removed. The muscle of the thigh and leg regions was then dissected to examine the femur, tibia and fibula bones under aseptic circumstances for macro-morphological evaluation. Then, left femurs were dehydrated in 100% ethanol for 48 h and dried at 100 °C for 24 h to measure dry weight of the whole bone. Subsequently, the bones were burned to ash at 600°C for 24 h with an electric furnace (Japan) to obtain ash weight of the whole bone [22].

Tissue preparation

The right femur of all rats was excised and trimmed from muscle attached or dissected appropriately. The samples were fixed in 10% neutral buffered formalin for 5 days, washed by tap water then they were decalcified. Decalcification process was carried by chelating agent (EDTA). The time for exposure to the decalcification varied so close monitoring of the process is needed. All samples were infiltrated with soft melted paraffin in a hot air oven and were embedded in hard paraffin forming paraffin blocks. The obtained sections were subjected to Harris's Hematoxylin and Eosin stain as a routine staining to demonstrate the general histological structure [23]. All the stained sections were examined with a standard light microscope (Olympus BX 21) and photographed at the Department of Histology and Cytology, Zagazig University.

The tibiae were cut apart, wrapped in labeled aluminum foil and kept at -80°C in order to prepare the bone homogenate. The samples were homogenized in phosphate buffered saline before being centrifuged at 1000 rpm for 20 min at 2-8 °C [24]. Following that, the supernatant was divided into two equal portions: one part used to assay gene expression and the second part for the peroxisome proliferator-activated receptors (PPAR- γ) assay, according to the manufacturer's instructions provided with Sandwich ELISA Kit (INOVA, Beijing, China), in terms of pg/mg protein[25].

Gene expression analysis

Using the real-time quantitative polymerase chain reaction, the expression patterns of mTORC1 and AMPK in bone supernatant were investigated (RT-qPCR). Trizol reagent was used to extract the total RNA (Thermo Fisher Scientific, Waltham, MA, USA). After that, complementary DNA (cDNA) was created in a 20 μL reverse transcription apparatus using 5 μL of total RNA that had been extracted.

Primers of upstream and downstream target genes (table 1) were added with 5 μL cDNA as a template. According to the instructions of the TaKaRa qRT-PCR reaction kit instruction (qRT-PCR; Takara, Shiga, Japan), The PCR dissolution curve was discovered and roughly quantified after the PCR reaction solution had been created. The internal reference was Glyceraldehyde 3-phosphate dehydrogenase (GAPDH). Thermo Fisher, USA's ABI 7500 Real-Time PCR System was used to examine the results [26].

Histomorphometric analysis:

Six animals per each group were used for the morphometrical analysis; the image J software (Fiji Image J; 1.51 n, NIH) was used for the quantitative measurements of area % of bone by using H&E-stained photomicrographs from the different three groups.

Statistical analysis:

All statistical analysis was achieved by Graph Pad prism 8.0.2 (Graph Pad Software, Inc). Firstly, data screened for normality by Shapiro-Wilk test and testing the equality of variance among the three groups performed by Bartlett's test. The data were normally distributed and homogeneity of variance was met. Data described as mean \pm SD. One-way ANOVA was run to test differences among group means followed by Tukey's multiple comparisons test. $P < 0.05$ considered the limit of significance.

RESULTS:

Effect of omentin-1 on metabolic measurements:

As depicted in Table 2, the results of this work showed a significant increase in BMI, glucose, insulin, HOMA-IR in HFD (IIa) and HFD+omentin-1 (IIb) subgroups (IIa) in comparison to control group (I) ($p < 0.05$). However, the previously mentioned parameters were significantly decreased in HFD+omentin-1 subgroup (IIb) in comparison to HFD subgroup (IIa) ($p < 0.05$).

Additionally, serum TC and TG in HFD group (IIa) ($p < 0.001$ and $p < 0.05$, respectively) and HFD+omentin-1 group (IIb) ($p < 0.01$ and $p < 0.05$, respectively) significantly increased in comparison to control group (I). However, the previously mentioned parameters were significantly decreased in HFD+omentin-1 group (IIb) in comparison to HFD group (IIa) ($p < 0.05$ and $p < 0.01$, respectively).

Effect of omentin-1 on bone morphology and measurements:

As shown in Table 3, there is no difference in macro-morphology in femur, tibia and fibula bones between obese and treated groups in comparison with control one (Figure 1).

It was noticed that dry and ash weight of left femur in the present work were significantly lower in HFD group (IIa) and HFD+omentin-1 group (IIb) when compared to control group ($p < 0.001$). However, both parameters were significantly higher in HFD+omentin-1 group (IIb) when compared to HFD group (IIa) ($p < 0.001$).

In addition, serum ALP in this study was significantly higher in HFD group (IIa) ($p < 0.01$) and HFD+omentin-1 group (IIb) ($p < 0.05$) when compared to control group. However, it was significantly lower in HFD+omentin-1 group (IIb) when compared to HFD group (IIa) ($p < 0.05$). However, serum Ca and IP showed insignificant changes among all study groups ($p > 0.05$).

Effect of omentin-1 on Serum GDF-11:

The results of the present work revealed that HFD significantly reduced GDF-11 in group (IIa) when compared to control group ($p < 0.001$). In addition, omentin-1 treatment significantly increased GDF-11 level in group (IIb) when compared to group (IIa) ($p < 0.05$). However, no significant change was observed between control group (I) and HFD+omentin-1 treated group (IIb) ($p > 0.05$) (Figure 2a).

Effect of omentin-1 on AMPK, mTORC1 gene expression and PPAR- γ bone content in different groups (Figure 2b, 2c, 2d).

In comparison to control rats in group (I), HFD-supplementation to group (IIa) showed significantly ($p < 0.001$) down-regulated AMPK gene expression, while up-regulated mTORC1 gene expression. On the other hand, omentin-1 administration to group (IIb) revealed significantly up-regulated AMPK gene expression in comparison with both HFD and control groups ($p < 0.001$). Moreover, omentin-1 treatment (group IIb) induced a significant down-regulation in mTORC1 gene expression when compared to HFD group (IIa) ($p < 0.001$) (Figure 2b, 2c). With regard to PPAR- γ , HFD rats (group IIa) displayed a significant increase in PPAR- γ bone level as compared to control group (I) ($p < 0.001$), while omentin-1 administration to rats in group (IIb) induced a significant decrease in PPAR- γ bone level in comparison with HFD group (IIa) ($p < 0.001$) (Figure 2d).

5. Effect of Omentin-1 on bone histopathological analysis

The microscopical examination of the femur bone of control group revealed that the cortical bone consisted of cellular lamellae of osteocytes inside their lacunae and several haversian canals (Fig. 3a). The head of femur bone composed of cancellous bone trabeculae inside the lumen forming some cavities containing bone marrow which consisted of hematopoietic tissue islands. The bony tissue was surrounded by an outer periosteum which composed of a dense connective tissue that covers the external surface of the bone and lined with an endosteum (Fig. 3b).

On longitudinal section of femur of obese group, it displayed that bone was surrounded by enormous amount of adipose tissue and the marrow cavities contained several adipocytes in comparison to other hematopoietic cells and in comparison, to the control group (Figure 4a). Whereas the head of femur bone showed severe thinning of bone with several trabeculae of cancellous bone forming meshwork of vascular sinuses containing hematopoietic tissue with abundant adipocytes. The bony tissue was lesser in amount compared to the control rats with several caveoli in between (Figure 4b).

The longitudinal section of the shaft of femur bone of omentin-1 treated obese group displayed higher amount of bony mass with more haversian canals than obese group (Figure 5a). However, its head showed solidifying and thickening of its cancellous bone trabeculae and some improvement represented by increase in bone mass with a network of trabecular sinuses (Figure 5b).

Statistically, the results showed that there is highly significant difference in the percentage of bone area among the three rat groups $p < 0.0001$. Obese group recorded the lowest percentage ($32.93 \pm 3.61b$) compared to control and treated groups. Percentage of bone area of treated group did not significantly differ than control group ($50.03 \pm 1.09a$ and $51.99 \pm 2.49a$, respectively) (Table 4 and Figure 6).

Regarding correlation coefficient between GDF-11 and bone parameters, it showed significant positive correlation with Dry weight in

HFD group and HFD+omentin-1 group ($p < 0.05$ and $p < 0.01$, respectively), ash weight ($p < 0.05$), and with Area % of bone in all groups ($p < 0.01$, 0.01 , and 0.001 , respectively). However, GDF-11 showed a significant negative correlation with ALP in all groups ($p < 0.01$, 0.001 , and 0.001 , respectively) (Table 5). While no significant correlation was found between GDF-11 and bone dry weight in control group ($p > 0.05$) or bone ash weight in control and HFD group (II) ($p > 0.05$) (Table 5).

Table 1: Primers of studied genes

Primers	
GAPDH	forward 5'-GGATGGAATTGTGAGGGAGA-3' reverse 5'-GTGGACCTCATGGCCTACAT-3'
mTORC1	forward, 5'-ATG ACG AGA CCC AGG CTA AG-3'; reverse, 5'-GCC AGT CCT CTA CAA TAC GC-3'.
AMPK	forward, 5'TGAAGCCAGAGAACGTGTTG-3', reverse 5'- ATAATTTGGCGATCCACAGC-3'

Table 2: Metabolic measurements in all groups

	Control group	Obese group	Omentin group
BMI (g/cm ²)	0.49± 0.04	0.76±0.04 ^{a*}	0.60 ±0.05 ^{a*b*}
Glucose (mg/dl)	93±6.7	187±8.9 ^{a*}	134±8.5 ^{a* b*}
Insulin (µIU/ml)	11.5± 1.4	21.5±3.7 ^{a*}	13.5±1.9 ^{a* b*}
HOMA-IR	2.64± 0.57	9.92±0.21 ^{a*}	4.47±0.31 ^{a* b*}
TC (mg/dl)	89.27± 10.6	152± 13.23 ^{a***}	102.5± 11.08 ^{a***b*}
TG (mg/dl)	67± 11.6	140.83± 1 1.59 ^{a*}	95.01 ±8.91 ^{a*b**}

(a)=Significant vs. group I. (b) =Significant vs. group IIa. *: $p < 0.05$, **: $p < 0.01$, ***: $p < 0.001$

Table 3: Bone weight and serum biochemical parameters in all groups

	Control group	Obese group	Omentin group
Dry weight (mg)	929 ± 84.1	792 ± 111.8 ^{a***}	820±113.6 ^{a***b***}
Ash weight (mg)	554 ± 70.3	434 ± 48.0 ^{a*}	534± 53.9 ^{a*b*}
Ca (mg/dl)	9.68±1.54	9.54±1.33	9.59±2.05
PI (mg/dl)	4.77±0.64	4.56±0.98	4.68±0.85
ALP(U/l)	40.9±3.5	75.9±7.5 ^{a**}	51.3±5.4 ^{a*b*}

(a)=Significant vs. group I. (b)=Significant vs. group IIa. *: $p < 0.05$, **: $p < 0.01$

Table 4: The mean values of Area % of bone of all study groups

Group	Area % of bone
Control	51.99 ±2.49
Obese group	32.93±3.61 ^{a*}
Omentin group	50.03±1.09 ^{b*}

(a)=Significant vs. group I. (b)=Significant vs. group IIa. *: $p < 0.05$

Table 5: Correlation coefficient between GDF-11 and bone parameters in all study groups

	Control group	Obese group	Omentin group
Dry weight	0.33 ^{ns}	0.75 [*]	0.78 ^{**}
Ash weight	0.48 ^{ns}	0.49 ^{ns}	0.70 [*]
ALP	-0.85 ^{**}	-0.90 ^{***}	-0.92 ^{***}
Area % of bone	0.84 ^{**}	0.81 ^{**}	0.92 ^{***}

*: $p < 0.05$, **: $p < 0.01$, ***: $p < 0.001$, ns: non-significant

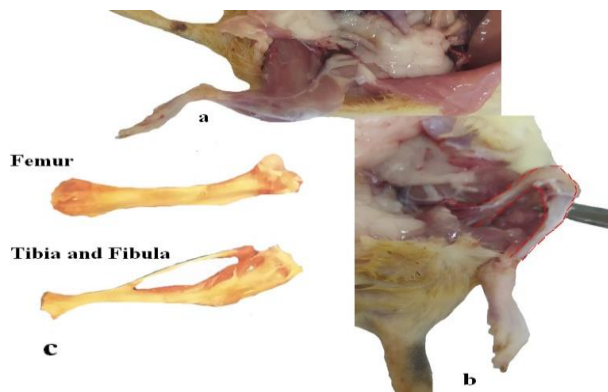


Figure 1: A photomicrograph of rat showing medial surface of thigh and leg regions of hind limb (a), dissection of hind limb to explore different bones (b) and femur, tibia and fibula of control group (c).

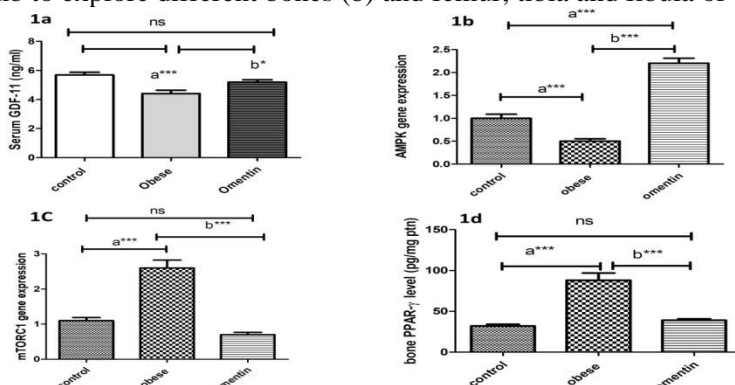


Figure 2: Bar charts representing mean \pm SD of a) serum level of growth differentiation factor-11 (GDF-11), b) AMPK gene expression, c) mTORC1 gene expression and d) PPAR- γ bone level in all study groups. (a):Significant vs. group I. (b):Significant vs. group IIa. *: $p < 0.05$, ***: $p < 0.001$, ns: non-significant.

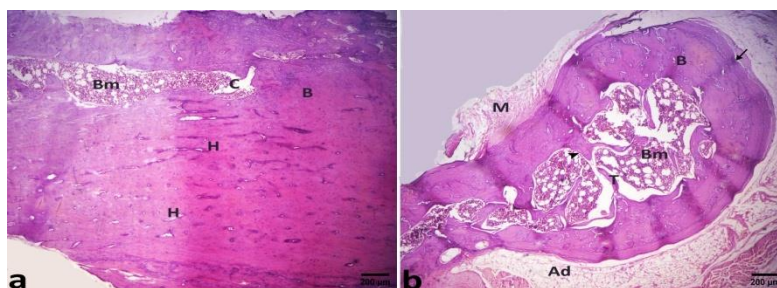


Fig 3:Photomicrograph of a decalcified long bone of control group stained with H and E showed: **a)** longitudinal section of bones showed bone tissue "B", Haversian canal "H", bone marrow cavity "C" and bone marrow "BM". **b)** head of femur bone showed skeletal muscle "M", Adipose tissue "Ad", periosteum "arrow", endosteum "arrowhead", bone tissue "B", bone marrow "BM" and cancellous bone trabeculae "T".

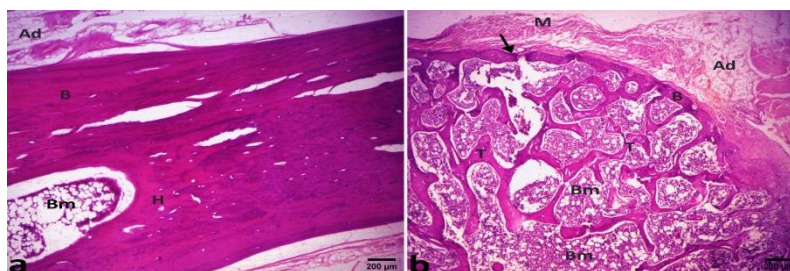


Figure 4:Photomicrograph of a decalcified long bone of obese group stained with H and E showed: **a)** longitudinal section of bones showed bone tissue "B", Haversian canal "H", Adipose tissue "Ad", and bone marrow with many adipocytes "BM". **b)** head of femur bone showed skeletal muscle "M", Adipose tissue "Ad", periosteum "arrow", bone tissue "B", bone marrow "BM", cancellous bone trabeculae "T".

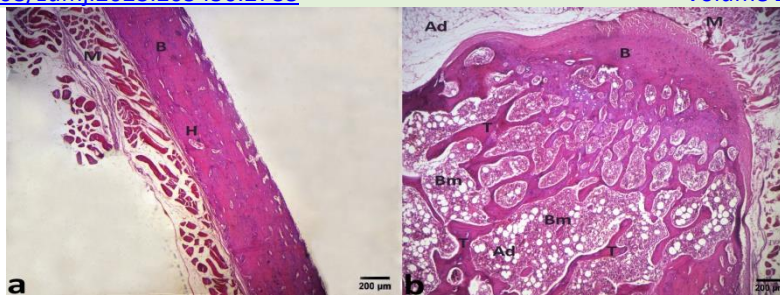


Figure 5: Photomicrograph of a decalcified long bone of omentin-1 treated obese group stained with H and E showed: **a)** longitudinal section of bones showed skeletal muscle "M", bone tissue "B" and Haversian canal "H". **b)** head of femur bone showed skeletal muscle "M", Adipose tissue "Ad", bone tissue "B", bone marrow "BM", cancellous bone trabeculae "T".

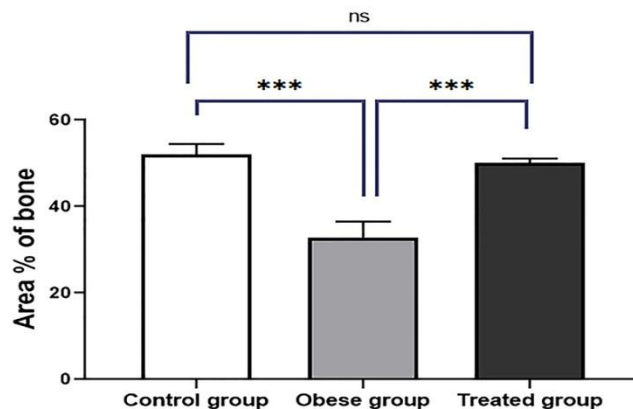


Figure 6: Bar chart showing the area percent of bone of control, obese and obese treated group; Data are expressed as means ± SD, (n = 6). ***means highly significant (p < 0.0001), ns means non significant.

DISCUSSION

It is believed that obesity is a major risk factor for osteoporosis and bone fractures compared to normal weight range. Data from animal models indicate that obesity has a negative impact on bone metabolism [27].

In the current study, we developed obesity in male albino rats by feeding them with HFD. HFD-induced obesity is considered the commonest model to assess the impact of adiposity on bone [28].

As anticipated, we observed that BMI, serum TGs and cholesterol levels were significantly increased in HFD rats. These parameters are well-accepted indicators of obesity in HFD rats. Our findings are in line with those of Malvi et al. [29]. Moreover, our results showed that diet-induced obesity caused hyperglycemia and increased insulin resistance in those rats when compared with animals in control group.

Interestingly, the current results revealed that HFD-rats treated with omentin-1 showed a significant decrease in BMI, serum TGs and cholesterol levels. Furthermore, omentin-1 administration prevented HFD-induced hyperglycemia, insulin resistance and osteoporosis in rats. In consistent with our results,

Lu et al. [30] displayed that omentin-1 improved metabolic homeostasis in obese rats. Omentin-1 is thought to exert its function in multiple organs, such as liver, muscle and adipose tissue, regulating glucose metabolism via enhancing insulin sensitivity. Moreover, omentin-1 expression in adipose tissue was found to have a negative correlation with obesity index and lipid metabolism parameters [31].

On a molecular level, our results showed that omentin-1 treatment increased AMP protein-kinase (AMPK) and decreased mammalian target rapamycin (mTORC1) expression, which was up-regulated in response to HFD. These data support a formal study of Wen et al. [32] who reported that mTOR activity is aberrantly elevated in obesity and is thought to regulate multiple metabolic pathways. In adipocytes, mTORC1 is suggested to have a crucial role in adipogenesis regulation and differentiation of preadipocyte into mature adipocytes. Furthermore, mTORC1 enhanced de novo lipogenesis through activation of S6 kinase (S6K), which phosphorylates the sterol regulatory element-binding proteins (SREBPs), the master regulator of lipid synthesis [33]. Additionally, Peterson et al. [34] found that mTORC1 could phosphorylate Lipin1, preventing

its translocation to nucleus and hence promoting SREBP1-mediated lipogenesis.

In a transgenic mouse model, Arif et al. [35] demonstrated that inhibition of mTORC1 signaling resulted in adipose tissue mass reduction and resistance to HFD-induced obesity. Accordingly, we suggest that omentin-1, by blunting mTORC1 signaling cascade through activating the upstream inhibitor AMPK, could abrogate HFD-induced obesity and hyperlipidemia.

Regarding glycemic control, omentin-1 is suggested to improve insulin sensitivity and enhance insulin-induced glucose transport via activation of AMPK, which in turn inhibited mTOR-p70S6K leading to increased activity of insulin receptor substrate (IRS). These data are consistent with those of Escoté et al. [36]. It is noteworthy that chronic mTOR activation results in insulin resistance and contributes to development of metabolic diseases such as diabetes [37]. Upon activation of mTORC1, S6K1 directly phosphorylates IRS and promotes its degradation, with subsequent impairment of insulin mediated PI3K/AKT stimulation and its downstream effects for instance uptake of glucose and synthesis of glycogen [33]. Therefore, it has been recommended that inhibition of the mTOR pathway is a potential therapeutic target to counteract insulin resistance and improve glucose homeostasis [38].

In the current investigation, we clearly observed the negative effect of obesity on bone and noted a significant bone loss in obese rats displayed by reduction in bone weight and increase in ALP activity. Additionally, histopathological study of the femurs of obese rats showed severe thinning of cortical bone, several trabeculae of cancellous bone with abundant adipocytes, lesser amount of bony tissue surrounded by enormous amount of adipose tissue with several adipocytes in the marrow cavities. On the other hand, omentin-1 treatment was found to reverse the previously mentioned osteoporotic changes. This improvement was evidenced histopathologically as there was solidification of cortical bone, enormous increase in bone mass as well as an increase in dry and ash weight of left femur. Moreover, omentin-1 was found to significantly decrease ALP activity. These data were in agreement with those of Tang et al. [12] who established that omentin-1 is able to stimulate both osteoblastic differentiation and viability, promoting bone formation and preventing osteoporosis.

Adipocytes and osteoblasts both arise from the same bone marrow mesenchymal stem cell progenitors. Meanwhile, there is a reciprocal association between the osteoblastic and adipogenic differentiation. It has been postulated that obesity induces adipocyte differentiation and lipid accumulation in the body, while reduces the osteoblast differentiation [28]. That imbalance in bone homeostasis caused by impaired osteoblastogenesis and increased adipogenesis may result in reduced bone formation, bone mass loss, bone marrow fat accumulation and ultimately osteoporosis [27]. Therefore, inhibition of adipogenic differentiation in bone marrow while simultaneously promoting osteogenesis may be a therapeutic approach for osteoporosis [7]. Importantly, mTOR signaling has been revealed to associate with bone loss [39]. Therefore, we suggest that the observed anti-osteoporotic effect of omentin-1 can be partially attributed to down-regulation of mTORC1. Our notion is supported by previous reports which showed that suppression of mTOR signaling by rapamycin could stimulate osteoblast differentiation of human embryonic stem cells. Furthermore, inhibition of mTOR signaling could reduce osteoclasts differentiation, proliferation and survival [40]. In contrast to our findings, it has been discovered that activation of mTOR signaling enhanced osteoblastic differentiation [41]. Additionally, sirolimus, an inhibitor of mTOR signaling, was reported to suppress osteogenic differentiation of human bone marrow-derived mesenchymal stem cells (BMSCs) and osteoblasts (MG63 cells) [42].

In this investigation, we detected that omentin-1 treated rats showed a significant suppression of nuclear receptor peroxisome proliferator-activated receptor- γ (PPAR- γ) along with mTORC1 down-regulation. This effect could provide another mechanism of omentin-1 anti-osteoporotic effect though blunting adipogenesis. In line with our results, Shen et al. [7] postulated that mTORC1 plays a critical role in PPAR- γ -mediated adipogenesis. As a transcription factor, PPAR- γ can indirectly reduce osteoblastic differentiation in BMSCs via stimulating adipogenesis; due to the reciprocal relationship between osteoblastic and adipogenic differentiation.

Moreover, PPAR- γ was reported to modulate osteogenesis directly in mouse and human osteoblasts. In transgenic mice over-expressing PPAR- γ in osteoblast, it was observed that PPAR- γ induced osteoblasts trans-differentiation into adipocytes [34]. Meanwhile, in

vitro studies revealed that the mTOR inhibitors could impair the differentiation of preadipocyte to mature adipocytes via PPAR- γ inhibition. Similarly, in vivo rapamycin treatment reduces adipose tissue expression of several PPAR- γ target genes [43]. Those aforementioned evidences point to a possible cross-talk between PPAR- γ and mTORC1 and emphasize the vital function of mTORC1/ PPAR- γ signaling in maintaining bone homeostasis.

Taken together, the above-mentioned data support our hypothesis that the beneficial anti-osteoporotic effect of omentin-1 can be attributed to AMPK/mTORC1/PPAR- γ pathway.

Importantly, the results of the current work displayed that GDF-11 level was elevated following omentin-1 treatment. Moreover, GDF-11 was positively correlated with bone weight and area percentage of bone. In addition, GDF-11 showed a significant negative correlation with ALP in all groups. According to our observations, we suggest that the exhibited beneficial effects of Omentin-1 can be enhanced by GDF-11. In line with our findings, Zhang et al.[44]reported that circulating GDF-11 levels were significantly diminished in both aged humans and patients with osteoporosis, and GDF-11 expression levels were substantially down-regulated in the bone marrow of mice with osteoporosis. Additionally,Suhand Lee.[45] revealed that treatment of BMSCs with recombinant GDF-11 proteins significantly promoted osteoblast differentiation and inhibited adipogenesis, highlighting the pro-osteogenic effect of GDF-11. On the contrary, Liu et al. [46] found that treatment with recombinant GDF-11 caused bone loss in both young and old mice by impairing osteoblast differentiation and increasing osteoclast formation. Additionally, higher circulating levels of GDF-11 were interrelated to lower BMD in postmenopausal women, suggesting that GDF-11 has an inhibitory influence on bone formation [47].

Importantly, we found a molecular cross talk between omentin-1 and GDF-11. Our notion is supported by a former study of Day et al.[48], who demonstrated that GDF-11 induced the phosphorylation of AMPK through the non-canonical GDF-11 signaling cascades PI3K/AKT and AMPK, which is hypothesized to affect metabolic homeostasis. In obese mice and mice with STZ-induced diabetes, GDF-11 over expression via gene transfer has been shown to prevent HFD-induced obesity, enhance islet β -cell function, regulate glucose homeostasis and lipid metabolism [49].Moreover, Zhang et al. [50]

showed that GDF-11, by inhibiting PPAR- γ activity, could boost osteoblast genesis.

The present study showed some limitations as the small sample size, the consistent age of animals as this limit the possibility of generalization of the results to all age groups, in addition, there is a lack to serum omentin level; subsequently, there might be a potential perplexing factor.

CONCLUSION

In conclusion, our findings demonstrate that omentin-1 plays an essential role in maintenance of metabolic homeostasis and is able to alleviate osteoporotic bone loss induced in rats subjected to HFD regimen through AMPK/mTORC1/PPAR- γ pathway. Furthermore, our study suggests a potential cross talk between omentin-1 and GDF-11.Taken together, these data suggest that omentin-1 may serve as a novel therapeutic target for obesity induced metabolic and bone disorders.

Acknowledgment: For supporting this effort by providing the necessary kits, chemicals, and tools are the Ministry of Higher Education and Scientific Research and the Faculty of Medicine at Zagazig University in Egypt. All experiments were conducted in the labs of the Medical Physiology and Biochemistry departments at Zagazig University's Faculty of Medicine. We extend our thanks to Dr. Nora Mustafa, biochemistry lecturer, Faculty of Medicine, Zagazig University, for completing the work of the genetics study.

Conflict of Interests: The authors declare no competing interests.

Funding information: no fund was received from any agency.

REFERENCES

1. Fassio A, Idolazzi L, Rossini M, Gatti D, Adami G, Giollo A, et al. The obesity paradox and osteoporosis. *Eat Weight Disord.* 2018;23(3):293–302.
2. Compston JE, McClung MR, Leslie WD. Osteoporosis. *Lancet*, 2019; 393(10169):364–76.
3. Mangion D, Pace NP, Formosa MM. The relationship between adipokine levels and bone mass-A systematic review. *Endocrinol Diabetes Metab.* 2023;6(3):e408. doi: 10.1002/edm2.408. Epub 2023 Feb 9. PMID: 36759562; PMCID: PMC10164433..
4. Chen G, Deng C, Li YP. TGF-beta and BMP signaling in osteoblast differentiation and bone formation. *Int J Biol Sci.* 2012;8(2):272–88.
5. Stanfel MN, Shamieh LS, Kaerberlein M, Kennedy BK. The TOR pathway comes of age. *Biochimica et BiophysicaActa.* 2009;1790(10):1067–1074.
6. Zheng X, Boyer L, JinM, Kim Y, Fan W, Bardy C, et al.Alleviation of neuronal energy deficiency by

- mTOR inhibition as a treatment for mitochondria-related neurodegeneration. *Elife*, 2016; 5: e13378.
7. Shen G, Ren H, Qiu T, Zhang Z, Zhao W, Yu X, et al. Mammalian Target of Rapamycin As a Therapeutic Target in Osteoporosis. *J Cell Physiol*. 2018;233(5):3929-3944. doi: 10.1002/jcp.26161.
 8. Wang P, Abdin E, Shafie S, Chong SA, Vaingankar JA, Subramaniam M. Estimation of prevalence of osteoporosis using OSTA and its correlation with sociodemographic factors, disability and comorbidities. *International Journal of Environmental Research and Public Health*, 2019; 6(13): 2338.
 9. Xie H, Xie PL, Luo XH, Wu XP, Zhou HD, Tang SY, et al. Omentin-1 exerts bonesparing effect in ovariectomized mice. *Osteoporosis International*, 2012; 23(4): 1425–1436.
 10. Yan P, Xu Y, Zhang Z, Zhu J, Miao Y, Gao C, et al. Association of Circulating Omentin-1 with Osteoporosis in a Chinese Type 2 Diabetic Population. *Mediators of Inflammation*, 2020;2020: Article ID 9389720, 16 pages <https://doi.org/10.1155/2020/9389720>.
 11. Yang L, Zhao XL, Liao B, Qin AP. Relationships between serum omentin-1 levels and bone mineral density in older men with osteoporosis. *Chronic Diseases and Translational Medicine*, 2016; 2(1):48–54.
 12. Tang C, Liang D, Qiu Y, Zhu J, Tang G. Omentin-1 induces osteoblast viability and differentiation via the TGF- β /Smad signaling pathway in osteoporosis. *Mol Med Rep*. 2022; 25(4):132. doi: 10.3892/mmr.2022.12648.
 13. Walker RG, Poggioli T, Katsimpardi L, Buchanan SM, Oh J, Wattrus S, et al. Biochemistry and biology of GDF11 and myostatin: similarities, differences, and questions for future investigation. *Circ Res*. 2016;118(7):1125–42.
 14. Lu B, Zhong J, Pan J, Yuan X, Ren M, Jiang L, et al. Gdf11 gene transfer prevents high fat diet-induced obesity and improves metabolic homeostasis in obese and STZ-induced diabetic mice. *J Transl Med*. 2019;17(1):422. doi: 10.1186/s12967-019-02166-1.
 15. Fraulob JC, Ogg-Diamantino R, Fernandessantos C, Aguila M.B. A Mouse Model of Metabolic Syndrome: Insulin Resistance, Fatty Liver and Non-Alcoholic Fatty Pancreas Disease (NAFPD) in C57BL/6 Mice Fed a High Fat Diet. *J. Clin. Biochem. Nutr*.2010; 46 (3): 212-23.
 16. Brunetti L, Orlando G, Ferrante C, Recinella L, Leone S, Chiavaroli A, et al. Orexigenic effects of omentin-1 related to decreased CART and CRH gene expression and increased norepinephrine synthesis and release in the hypothalamus. *Peptides*. 2013;44:66-74. DOI: 10.1016/j.peptides.2013.03.019.
 17. Novelli E, Diniz Y, Galhardi C, Ebaid G, Rodrigues H. Anthropometrical parameters and markers of obesity in rats. *Laboratory Animals*.2007;41: 111-119.
 18. Tietz NW, Cook T, Mcniven MA. *Clinical Guide to Laboratory Tests*; W.B. Saunders: Philadelphia, pp. 509-512, 1995.
 19. Temple RC, Clark PM, Hales CN. Measurement of insulin secretion in type 2 diabetes: Problems and pitfalls. *Diab Med*. 1992;9:503-551.
 20. Farley JR, Jorch UM. Differential effects of phospholipids on skeletal alkaline phosphatase activity in extracts, in situ, and in circulation. *Arch Biochem Biophys*. 1983;221:477-488.
 21. Juan A-H, Victoria C, Amaia R, Beatriz R, Camilo S, Juan G, et al. Circulating GDF11 levels are decreased with age but are unchanged with obesity and type 2 diabetes. *Aging*, 2019;11. 10.18632/aging.101865.
 22. Minematsua A, Nishiia Y, Sakata S. High-fat/high-sucrose diet results in higher bone mass in aged rats. *Bone Reports*, 2018;8:18–24.
 23. Suvarna KS, Layton C, John D. Bancroft's theory and practice of histological Techniques 8th ed., Churchill Livingstone, New York, London, 2018, Ch. 6: 73-96, Ch. 10: 126-139, Ch. 17: 286-300.
 24. Hamza S, Fathy S, EL-Azab S. Effect of diode laser biostimulation compared to Teriparatide on induced osteoporosis in rats: an animal study from Egypt. *Int J Clin Exp Pathol*. 2020; 13(8): 1970–1985.
 25. Saleh RS, Ghareeb AD, Masoud AA, Sheta E, Nabil M, Masoud MI, et al. Phoenix dactylifera L Pits Extract Restored Bone Homeostasis in Glucocorticoid-Induced Osteoporotic Animal Model through the Antioxidant Effect and Wnt5a Non-Canonical Signaling. *Antioxidants*, 2022; 11:508. <https://doi.org/10.3390/antiox11030508>
 26. Men Z, Huang C, Xu M, Ma J, Wan L, Huang J, et al. Zhuangu Zhitong Capsule alleviates postmenopausal osteoporosis in ovariectomized rats by regulating autophagy through AMPK/mTOR signaling pathway. *Ann Transl Med*. 2022;10(16):900 | <https://dx.doi.org/10.21037/atm-22-3724>
 27. Roy B, Curtis EM, Fears SL, Nahashon NS, Fentress MH. Molecular Mechanisms of Obesity-Induced Osteoporosis and Muscle Atrophy. *Frontiers in Physiology* | www.frontiersin.org. 2016; 7:Article439.
 28. Gkastaris K, Goulis GD, Potoupnis M, Anastasilakis DA, Kapetanios G. Obesity, osteoporosis and bone metabolism. *J Musculoskelet Neuronal Interact*. 2020; 20(3):372-381.
 29. Malvi P, Piprode V, Chaube P, Pote TS, Mittal M, Chattopadhyay N, et al. High fat diet promotes achievement of peak bone mass in young rats. *Biochemical and Biophysical Research Communications*, 2014; 455: 133–138.
 30. Lu Q, Tu M-L, Li C-J, Zhang L, Jiang T-J, Liu T, et al. GDF11 inhibits bone formation by activating Smad2/3 in bone marrow mesenchymal stem cells. *Calcif. Tissue Int*. 2016; 99:500–509.
 31. Sperling M, Grzelak T, Pelczyńska M, Bogdański P, Formanowicz D, Czyżewska K. Association of Serum Omentin-1 Concentration with the Content of Adipose Tissue and Glucose Tolerance in

- Subjects with Central Obesity. *Biomedicines*, 2023; 11(2):331. <https://doi.org/10.3390/biomedicines11020331>.
32. Wen X, Zhang B, Wu B. Signaling pathways in obesity: mechanisms and therapeutic interventions. *Sig Transduct Target Ther*, 2022; 7:298.
33. Mao Z, Zhang W. Role of mTOR in Glucose and Lipid Metabolism. *Int J Mol Sci*. 2018; 19:2043; doi:10.3390/ijms19072043
34. Peterson TR, Sengupta SS, Harris TE, Carmack AE, Kang SA, Balderas E, et al. mTOR complex 1 regulates lipin 1 localization to control the SREBP pathway. *Cell*, 2011; 146(3): 408-20.
35. Arif A, Terenzi F, Potdar AA, Jia J, Sacks J, China A, et al. EPRS is a critical mTORC1-S6K1 effector that influences adiposity in mice. *Nature*, 2017; 542:357-361.
36. Escoté X, Gómez-Zorita S, López-Yoldi M, Milton-Laskibar I, Fernández-Quintela A, J. Martínez A, et al. Role of Omentin, Vaspin, Cardiostrophin-1, TWEAK and NOV/CCN3 in Obesity and Diabetes Development. *Int. JMol Sci*. 2017; 18: 1770. doi:10.3390/ijms18081770
37. Laplante M, Sabatini DM. mTOR signaling in growth control and disease. *Cell*, 2012; 149:274-293. doi:10.1016/j.cell.2012.03.017
38. Ong SP, Wang ZL, Dai X, Tseng HS, Loo JS, Judicious SG. Toggling of mTOR Activity to Combat Insulin Resistance and Cancer: Current Evidence and Perspectives. *Front Pharmacol*. 2016; 7:395. doi: 10.3389/fphar.2016.00395
39. Tchetina EV, Maslova KA, Krylov MY, Myakotkin VA. Association of bone loss with the upregulation of survival-related genes and concomitant downregulation of Mammalian target of rapamycin and osteoblast differentiation-related genes in the peripheral blood of late postmenopausal osteoporotic women. *J Osteoporos*, 2015; 2015:802694.
40. Darcy A, Meltzer M, Miller J, Lee S, Chappell S, VerDonck K, et al. A novel library screen identifies immunosuppressors that promote osteoblast differentiation. *Bone*, 2012; 50(6):1294-303.
41. Feng X, Huang D, Lu X, Feng G, Xing J, Lu J, et al. Insulin like growth factor 1 can promote proliferation and osteogenic differentiation of human dental pulp stem cells via mTOR pathway. *Development, Growth and Differentiation*, 2014; 56(9):615-624.
42. Faghihi F, Baghaban EM, Nekookar A, Najar M, Salekdeh GH. The effect of purmorphamine and sirolimus on osteogenic differentiation of human bone marrow-derived mesenchymal stem cells. *Biomedicine and Pharmacotherapy*, 2013; 67(1): 31-38.
43. Hadji P, Coleman R, Gnant M. Bone effects of mammalian target of rapamycin (mTOR) inhibition with everolimus. *Crit Rev Oncol Hematol*. 2013; 87(2):101-111.
44. Zhang Y, Shao J, Wang Z, Yang T, Liu S, Liu Y, et al. Growth differentiation factor 11 is a protective factor for osteoblastogenesis by targeting PPAR γ . *Gene*. 2015; 557: 209-214.
45. Suh J and Lee Y-S. Similar sequences but dissimilar biological functions of GDF11 and myostatin. *Experimental & Molecular Medicine*, 2020; 52:1673-1693 <https://doi.org/10.1038/s12276-020-00516-4>
46. Liu W, Zhou L, Zhou C, Zhang S, Jing J, Xie L, et al. GDF11 decreases bone mass by stimulating osteoclastogenesis and inhibiting osteoblast differentiation. *Nat. Commun*. 2016; 7:12794 (2016).
47. Chen Y, Guo Q, Zhang M, Song S, Quan T, Zhao T, et al. Relationship of serum GDF11 levels with bone mineral density and bone turnover markers in postmenopausal Chinese women. *Bone Res*. 2016; 4:16012 (2016).
48. Day EA, Ford RJ, Steinberg GR. AMPK as a therapeutic target for treating metabolic diseases. *Trends Endocrinol Metab*. 2017; 28(8):545-60. <https://doi.org/10.1016/j.tem.2017.05.004>.
49. Seong HA, Manoharan R, Ha H. Smad proteins differentially regulate obesity-induced glucose and lipid abnormalities and inflammation via class-specific control of AMPK-related kinase MPK38/MELK activity. *Cell Death Dis*. 2018; 9(5):471. <https://doi.org/10.1038/s41419-018-0489-x>.
50. Zhang Y, Wei Y, Liu LFD, Li X, Pan L, Pang Y, et al. Role of growth differentiation factor 11 in development, physiology and disease. *Oncotarget*, 2017; 14; 8(46):81604-81616.

To Cite:

El-Malkey, N., Elwany, N., Goda, -, Aref, M., Khalil, S. Omentin -1 antagonizes high fat-induced bone loss in rats and promotes bone growth via AMPK/mTORC1/ PPAR- γ and GDF-11 signaling pathway. *Zagazig University Medical Journal*, 2023; (1124-1134): -. doi: 10.21608/zumj.2023.205450.2788